Water Practice & Technology

IWA PUBLISHING

Water Practice & Technology Vol 17 No 6, 1332 doi: 10.2166/wpt.2022.058

A kinetic, isotherm adsorption, and thermodynamic study of Congo red coagulation using *Leucaena* crude extract as natural coagulant

Hans Kristianto *, Natasa Manurung, Irene Kusuma Wardhani, Susiana Prasetyo, Asaf K. Sugih and Ariestya A. Arbita

Department of Chemical Engineering, Faculty of Industrial Technology, Parahyangan Catholic University, Ciumbuleuit 94, Bandung, West Java 40141, Indonesia
*Corresponding author. E-mail: hans.kristianto@unpar.ac.id

HK, 0000-0003-4747-4361; AAA, 0000-0003-0971-2963

ABSTRACT

The utilization of various natural resources as coagulant to treat various types of water and wastewater has seen considerable growth in recent years. The coagulation mechanism of natural coagulant is commonly charge neutralization followed by adsorption during the floc growth. However, due to lack of information, further investigation into the nature of the coagulation mechanism is needed. In this study, the coagulation of Congo red synthetic wastewater using crude leucaena extract was investigated at various initial Congo red concentrations (50–100 mg/L) and coagulation temperatures ranging from 30 to 50 °C. Furthermore, the nature of coagulation was investigated using various adsorption isotherms (the Langmuir, Freundlich, Temkin, and Brunauer-Emmet-Teller models) and kinetic models (pseudo-first, pseudo-second, Elovich, and intraparticle models). It was found that the Congo red concentrations, coagulation temperatures, and their interaction are significant to the dye removal. The sedimentation was well described by the pseudo-second order kinetic model, and the coagulation process followed the Langmuir isotherm. This indicates that the coagulation process involved chemisorption with monolayer formation on the coagulant. Moreover, the thermodynamic study shows that the coagulation was both endothermic and spontaneous.

Key words: Congo red, isotherm adsorption, kinetic, leucaena, natural coagulant, thermodynamic

HIGHLIGHTS

- Crude protein was extracted from *Leucaena leucocephala*.
- The Congo red coagulation followed Langmuir isotherm model.
- The settling kinetic followed the pseudo-second order kinetic model.
- The coagulation using leucaena crude extract was endothermic and spontaneous nature.

GRAPHICAL ABSTRACT

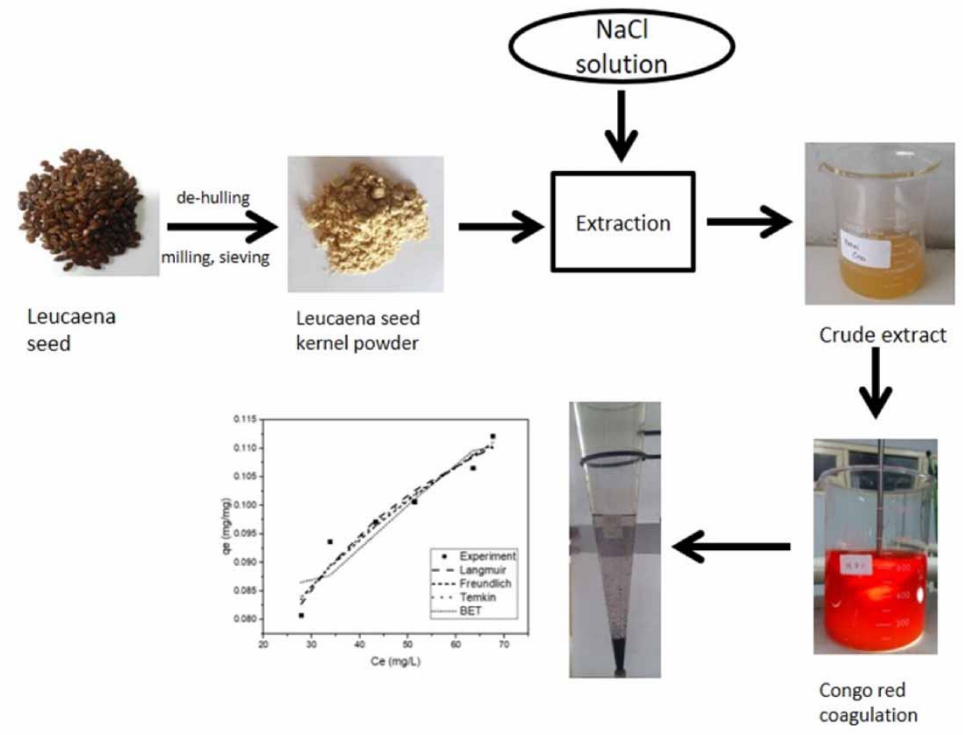

INTRODUCTION

Coagulation and flocculation are commonly employed technologies in water and wastewater treatment. There are some well-known advantages of coagulation and flocculation such as the simplicity of the process, commercially available chemicals, low equipment cost, and its ability to reduce contaminants (chemical oxygen demand, biochemical oxygen demand, organic content, and the like) (Crini & Lichtfouse 2019). The chemicals that are used as coagulant and flocculant can be classified as inorganic salts, such as aluminium sulphate, ferric chloride, ferric sulphate, ferrous sulphate; inorganic polymers, such as polyaluminium chloride, polyferric chloride, polyaluminium sulphate, and polyaluminium ferric chloride; and organic polymers, for example amino methyl polyacrylamide, polyamine, and polyethylenimine (Verma *et al.* 2012; Lal & Garg 2017, 2019). However, application of these coagulants poses some drawbacks such as their negative impact on human health, production of non-biodegradable sludge in high volume, and decrease of the water's pH after treatment (Yin 2010). Thus, alternative coagulants are needed to cope with these specific drawbacks.

In recent years, there has been an increasing trend in the investigation of utilizing natural-based coagulants to treat various water and wastewater. Generally, natural coagulants could be classified by their active coagulating agent, namely protein, polysaccharides, and polyphenols. These active coagulating agents are isolated from plants (seeds, fruits, leaves, roots) and animals, as well as microorganisms. Several studies recently reported on *Azadirachta indica* (Ahmad *et al.* 2021), *Hibiscus esulentus L.* (Okolo *et al.* 2021), *Azadirachta indica A. Juss.* (Thirugnanasambandham & Karri 2021), and *Moringa oleifera* (Yamaguchi *et al.* 2021). The application of natural coagulants in water and wastewater treatment brings some advantages, namely being relatively cost-effective, accessible, and producing less sludge with biodegradable characteristics compared to chemical coagulants (Ang & Mohammad 2020). All these positive traits of natural coagulants reflect their potential as a promising green alternative to substitute chemical coagulants.

Previously, our research team applied leucaena seed (*Leucaena leucocephala*) as a natural coagulant to treat turbidity (Kristianto *et al.* 2018) and remove colour (Kristianto *et al.* 2020a, 2020b) from synthetic wastewater. Based on those studies, it was found that charge neutralization is the coagulation mechanism of leucaena protein. Furthermore, according to Beltran-Heredia, Sanchez-Martın (Beltran-Heredia *et al.* 2009) after charge neutralization, a complex between dye and coagulant is formed and followed by flocs formation via sorption mechanisms.

The adsorption process is the rate controlling step; thus, the coagulation process could be modelled using adsorption models. Considering this coagulation mechanism, a number of researchers have reported the application of adsorption isotherm and kinetic models to describe the coagulation process by both natural (Rani & Talikoti 2013; Menkiti *et al.* 2018; Ohale *et al.* 2020; Ejimofor *et al.* 2022; Kristianto *et al.* 2022) and inorganic coagulant (Hussain *et al.* 2013; Hossain *et al.* 2019; Ngteni *et al.* 2020; Wu *et al.* 2020). In recent research by Vishali, Mullai (Vishali *et al.* 2022), several isotherm adsorption models and kinetics were employed to describe coagulation process of synthetic paint wastewater by using saline extract of *Strychnos potatorum*, *Cactus opuntia* and *Portunus sanguinolentus*. It was found that the coagulant was heterogenous in nature with the monolayer adsorption process, indicated by the suitability of the data and model (Vishali *et al.* 2022). Another study by Nnaji, Anadebe (Nnaji *et al.* 2022) investigated the coagulation of Cibacron blue and dispersed red dye wastewater using *Luffa cylindrica* seed extract. It was discovered that the coagulation process followed the Freundlich isotherm and pseudo-second order kinetic model (Nnaji *et al.* 2022). The study of isotherm models is useful to provide insight into colloid and coagulant amalgamation, while kinetic and thermodynamic models are utilized to describe the coagulation behaviour (Yasin *et al.* 2020).

This study has investigated the effect of Congo red concentration and coagulation temperature on the Congo red removal. Congo red, an anionic azo dye, is used as a model substance of organic pollutants. Furthermore, for the first time, more insights into the leucaena extract coagulation mechanism were observed by various isotherm adsorption models, namely Langmuir, Freundlich, Temkin, and Brunauer-Emmett-Teller (BET). The sedimentation kinetic was also investigated by several adsorption kinetic models, namely pseudo-first and second order, Elovich, and intraparticle diffusion models. Finally, the thermodynamic properties of the Congo red coagulation using leucaena crude extract were determined as well.

METHODOLOGY

Coagulant preparation

Preparation of leucaena crude extract as natural coagulant was conducted by following previous studies (Kristianto *et al.* 2019; Kristanda *et al.* 2021). To summarize, dried leucaena seeds from a local market in Probolinggo, East Java were washed, oven dried (60 °C, 4 h), crushed, and sieved to obtain leucaena seed kernel powder. The seed kernel powder was subsequently extracted using a 1 M NaCl saline solution at pH 9.0 for 1 h. The seed cake was then separated from the extract and the filtrate was used as natural coagulant. The protein concentration in the extract was determined by using the Bradford method with bovine serum albumin (BSA) as the standard (Bradford 1976), thus the protein concentration was expressed as mg equivalent BSA per mL (mg eq BSA/mL). The extract was freshly made prior to each experiment to prevent any degradation during storage.

Jar test experiment

The coagulation study of Congo red was made by using a jar test apparatus equipped with a water bath and thermostat. Congo red solutions at various initial concentrations (50–100 mg/L) were prepared, and the pH was adjusted by using a 0.1 M HCl or NaOH solution. The coagulation pH was fixed at 3.0, which was found to be the best pH for coagulation of Congo red by using leucaena extract (Kristianto *et al.* 2019, 2020a, 2020b). The temperature of Congo red solutions was also adjusted according to the variations (30–50 °C), prior to coagulant addition. A total amount of 3 mL of leucaena crude extract was added to the Congo red solution, followed by rapid (200 rpm, 3 min) and slow mixing (60 rpm, 30 min). The mixture was subsequently left to settle for 60 min, during which a sample was taken and measured every 5 min. Determination of Congo red concentration was accomplished by using spectrophotometer visible (Thermoscientific Genesys 150) at Congo red maximum wavelength. All experiments were performed in duplicate.

Kinetic, isotherm adsorption, and thermodynamic model

The evaluation of the coagulation mechanism was evaluated by using several isotherm adsorption and kinetic models. The adsorption capacity (q, mg/mg eq BSA) is calculated by using Equation (1), where Co and Ct are initial Congo red concentration and concentration at a certain time (t, min), respectively; m is the mass of coagulant (mg eq BSA), and V (L) is the volume of Congo red solution. The q values at a certain time and equilibrium

are denoted as *qe* and *qt*, respectively.

$$q = \frac{(Ct - Co)}{m} \times V \tag{1}$$

The kinetic and isotherm models used in this study are presented in Tables 1 and 2, respectively.

Table 1 | Kinetic models and their linearized form

Model	Equation	Linearized equation
Pseudo-first order	$qt = qe(1 - e^{-k_1 t})$	$\ln(qe - qt) = \ln(qe) - k_1 t$
Pseudo-second order	$qt = \frac{k_2 q_e^2 t}{1 + k_2 qet}$	$\frac{t}{qt} = \frac{t}{qe} + \frac{1}{k_2 qe^2}$
Elovich	$qt = \frac{1}{b}\ln(abt)$	$qt = \frac{1}{b}\ln(ab) + \frac{1}{b}\ln(t)$
Intraparticle diffusion		$qt = k_d t^{\frac{1}{2}} + C$

Table 2 | Isotherm models and their linearized form

Isotherm	Equation	Linearized equation
Langmuir	$qe = \frac{K_L.qm.Ce}{1 + K_L.Ce}$ $R_L = \frac{1}{1 + K_L Ci}$	$\frac{Ce}{qe} = \frac{Ce}{qm} + \frac{1}{K_L.qm}$
Freundlich	$qe = K_F.Ce^{\frac{1}{n}}$	$\log(qe) = \log(K_F) + \frac{1}{n}.\log(Ce)$
Temkin	$qe = \beta.\ln(\alpha.Ce)$	$qe = \beta.\ln(\alpha) + \beta.\ln(Ce)$
Brunauer-Emmett-Teller (BET)	$qe = \frac{ACeXm}{(Ci - Ce)\left[1 + (A-1)\frac{Ce}{Ci}\right]}$	$\frac{Ce}{(Ci - Ce)qe} = \frac{(A-1)}{AXm}\frac{Ce}{Ci} + \frac{1}{AXm}$

Suitability of the models for the experimental data was evaluated by several parameters, namely R^2, χ^2 and sum of square error (SSE). The R^2 values are obtained from linearizing the experimental data according to the respective model, while the χ^2 and SSE values are calculated using Equations (2) and (3), respectively.

$$\chi^2 = \sum_{i=1}^{n} \frac{(q \text{ model} - q \text{ experiment})^2}{q \text{ experiment}} \tag{2}$$

$$SSE = \sum_{i=1}^{n} (q \text{ model} - q \text{ experiment})^2 \tag{3}$$

The thermodynamics properties of the coagulation experiment were calculated by using the Langmuir constant (K_L), as the most suitable isotherm model from the isotherm adsorption study. The K_L value was then converted into a dimensionless equilibrium constant (K°) value by using Equation (4) (Zhou & Zhou 2014; Lima *et al.* 2019). Based on the obtained K°, the Gibbs free energy ($\Delta G°$; kJ/mol) was calculated using Equation (5), where R is the universal gas constant (8.314 J/mol. K) and T (K) is the adsorption temperature. Furthermore, the enthalpy ($\Delta H°$; kJ/mol) and entropy ($\Delta S°$; kJ/mol. K) was calculated using Equation (6).

$$K^\circ = K_L\left(\frac{L}{mg}\right).1000\frac{mg}{g}.55.51\frac{mol}{L}.\text{Mr Congo red}\left(\frac{g}{mol}\right) \tag{4}$$

$$\Delta G^\circ = -R.T.\ln(K^\circ) \tag{5}$$

$$\ln(K^\circ) = \frac{-\Delta H^\circ}{R}.\frac{1}{T} + \frac{\Delta S^\circ}{R} \tag{6}$$

RESULTS AND DISCUSSION

Effect of Congo red concentration and temperature on Congo red removal

The effect of Congo red concentration and temperature on the Congo red is presented in Figure 1. Furthermore, the result of analysis of variance (ANOVA) in this study is presented in Table 3. It can be observed that Congo red concentration, coagulation temperature, and their interaction are significant to the Congo red removal with a confidence level of 95%. It can also be discerned that with the increase of Congo red concentration, the percentage removal was decreased with the same coagulant dosage. As the Congo red concentration increased, more colloid particles existed in the system. Thus, the coagulant became limited at higher colloid concentration, resulting in the decrease of percentage removal. A similar trend has been reported by previous researchers (Vishali & Karthikeyan 2018; Luo *et al.* 2019; Vishali *et al.* 2020). On the other hand, with the increase of operating temperature, the Congo red removal followed suit and increased as well. It is generally known that temperature can affect the viscosity and surface tension of the aqueous system. Furthermore, these physical parameters have a positive influence to the Brownian motion of the particles that lead to aggregation and floc formation (Fitzpatrick *et al.* 2004; He & Xie 2021). A similar trend has also been reported by previous researchers (Patel & Vashi 2012; Rodrigues *et al.* 2013; Mahmoudabadi *et al.* 2019).

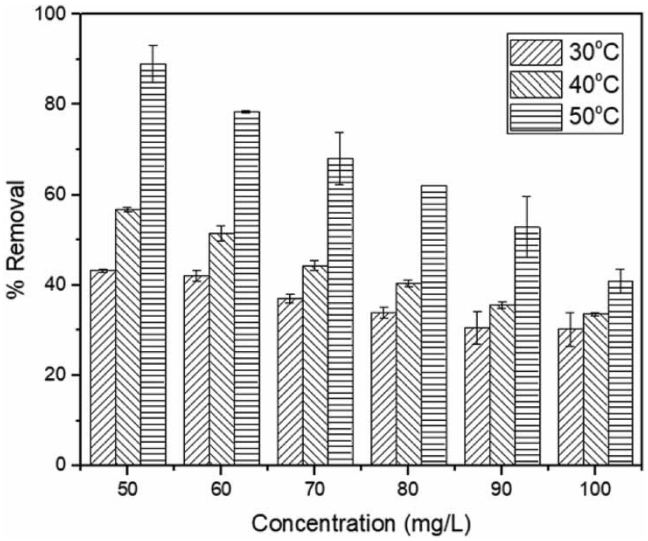

Figure 1 | Effect of concentration and temperature on % removal.

Table 3 | ANOVA for Congo red removal

Source	DF	Sum of Square	Mean Square	F	p
Concentration	5	3,366.23	673.25	86.9832	0.000
Temperature	2	5,452.64	2,726.32	352.2377	0.000
Concentration × Temperature	10	771.94	77.19	9.972868	0.000
Error	18	139.37	7.74		
Total	25	9,730.18			

S = 2.78259 R-Sq = 98.57% R-Sq(adj) = 97.21%.

Sedimentation kinetics

The profile of percentage removal at various initial concentrations and various temperatures is presented in Figure 2. It shows that similar percentage removal vs. time profile was observed from both figures, where a rapid increase of removal occurred during the initial 5 min, a further increase is observed until approximately

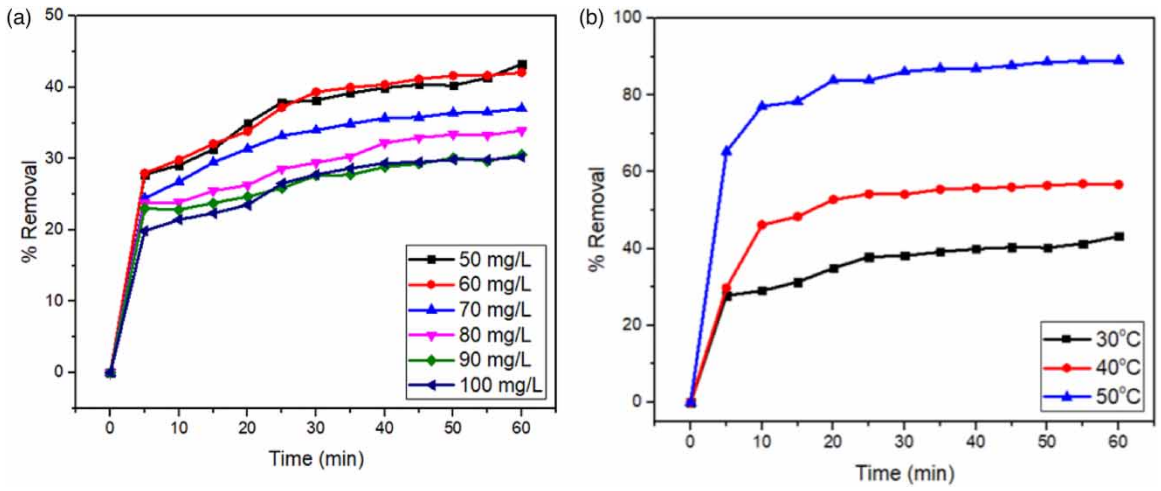

Figure 2 | Typical settling kinetic in various initial Congo red concentrations at 30 °C (a) and in various temperatures at initial concentration 50 mg/L (b).

40 min, and it becomes relatively constant until 60 min. The rapid removal increase at initial sedimentation time is due to the charge neutralization mechanism that is still dominant in this phase (Obiora-Okafo *et al.* 2020). After that, adsorption and flocs formation are the dominant steps that require more time to complete. The data obtained were then fitted to various kinetic models, namely pseudo-first order, pseudo-second order, Elovich, and intraparticle diffusion.

The pseudo-first order kinetic model assumes that the rate of adsorbate uptake per time is proportional to the difference of adsorption capacity that is usually suitable to describe the initial step of an adsorption process. Furthermore, the pseudo-first order kinetic model is usually suitable in a system with high initial adsorbate concentration and only a few active sites available on the adsorbate (Wang & Guo 2020). The parameters of the pseudo-first order kinetic model obtained in this study are presented in Table 4. Based on the evaluation of the model's suitability, it can be observed that this model generally has a good R^2 value, ranging from 0.74 to 0.97. However, the low suitability of the *qt* model compared to the experimental data is shown by the relatively high χ^2 and SSE value.

Table 4 | Parameters for pseudo-first order kinetic

		Initial concentration (mg/L)					
T (°C)	Parameter	50	60	70	80	90	100
30	k_1 (/min)	0.0478	0.0787	0.0701	0.0675	0.0592	0.0785
	qe (mg/mg)	0.0453	0.0703	0.0618	0.0731	0.0620	0.0871
	R^2	0.9387	0.9037	0.9269	0.9712	0.9071	0.9225
	χ^2	0.2266	0.0918	0.1836	0.1235	0.2688	1.0578
	SSE	0.0150	0.0071	0.0151	0.0101	0.0243	0.1050
40	k_1 (/min)	0.9739	0.9705	0.884	0.9598	0.9058	0.9462
	qe (mg/mg)	0.0692	0.0744	0.0582	0.0852	0.1502	0.0741
	R^2	0.0518	0.0075	0.0062	0.0000	0.0165	0.0005
	χ^2	0.1402	0.1915	0.3794	0.1334	0.1040	1.1499
	SSE	0.0130	0.0188	0.0364	0.0128	0.0107	0.1234
50	k_1 (/min)	0.0923	0.0812	0.0769	0.0825	0.0559	0.0904
	qe (mg/mg)	0.0907	0.1080	0.1497	0.1534	0.1250	0.1917
	R^2	0.9453	0.9711	0.9324	0.9798	0.8931	0.7242
	χ^2	0.5263	0.4316	0.1298	0.1304	0.3283	1.4546
	SSE	0.0853	0.0710	0.0191	0.0206	0.0495	0.2057

The pseudo-second order kinetic model is suitable to describe the adsorption process at low adsorbate concentration and adsorbent with abundant active sites on its surface (Wang & Guo 2020). The adsorption process is assumed to be second order with chemical sorption as the rate determining step. The chemical sorption happens

due to the high content of active sites and their interaction with adsorbate via covalent forces and electron exchange (Qiu *et al.* 2009). The parameters of the pseudo-second order kinetic model are presented in Table 5. It can be seen that this model is highly suitable for the experimental data, as shown in high R^2 (0.99) and low χ^2 and SSE values.

Table 5 | Parameters of pseudo-second order kinetic model

		Initial concentration (mg/L)					
T (°C)	Parameter	50	60	70	80	90	100
30	k_2 (mg/mg. min)	3.1997	2.7986	3.1302	2.3169	2.7351	2.1317
	qe (mg/mg)	0.0821	0.0982	0.1007	0.1049	0.1092	0.1182
	R^2	0.9927	0.9942	0.9963	0.9902	0.9931	0.9923
	χ^2	0.0023	0.0026	0.0014	0.0051	0.0047	0.0040
	SSE	0.0001	0.0002	0.0001	0.0004	0.0004	0.0003
40	k_2 (mg/mg. min)	3.5101	2.9156	2.6704	1.3347	1.9026	2.0745
	qe (mg/mg)	0.1093	0.1187	0.1158	0.1274	0.1254	0.1274
	R^2	0.9972	0.9970	0.9951	0.9875	0.9932	0.9940
	χ^2	0.0051	0.0013	0.0021	0.0067	0.0038	0.0027
	SSE	0.0003	0.0001	0.0002	0.0003	0.0003	0.0002
50	k_2 (mg/mg. min)	3.7192	2.2636	1.3403	1.2468	1.2286	1.1421
	qe (mg/mg)	0.1794	0.1914	0.1956	0.2061	0.1944	0.1738
	R^2	0.9992	0.9981	0.9939	0.9949	0.9918	0.9903
	χ^2	0.0008	0.0015	0.0026	0.0044	0.0041	0.0042
	SSE	0.0001	0.0002	0.0004	0.0006	0.0006	0.0004

The Elovich kinetic model is based on assumptions that the activation energy increases with adsorption time and adsorption occurs on heterogeneous adsorbents (Wang & Guo 2020). The Elovich model is usually useful to describe the phenomenon of adsorption. The parameters of the Elovich model are presented in Table 6. The small a values ($a < 1$) indicated a homogenous adsorbent of the natural coagulant, while large values of b ($b > 1$) suggested the occurrence of chemisorption in this study (Vishali & Karthikeyan 2018).

Table 6 | Parameters of Elovich model

		Initial concentration (mg/L)					
T (°C)	Parameter	50	60	70	80	90	100
30	a (mg/min mg)	0.0321	0.0389	0.0423	0.0432	0.0525	0.0450
	b (mg/mg)	56.8182	47.3934	46.2963	45.8716	44.6429	39.3701
	R^2	0.9336	0.9328	0.9261	0.9121	0.8769	0.9368
	χ^2	0.0043	0.0134	0.0055	0.0072	0.0095	0.0062
	SSE	0.0002	0.0010	0.0004	0.0005	0.0008	0.0005
40	a (mg/min mg)	0.0433	0.0497	0.0456	0.0320	0.0412	0.0477
	b (mg/mg)	40.6504	38.6100	39.5257	33.8983	35.7143	36.2319
	R^2	0.9209	0.9269	0.9359	0.9810	0.9653	0.9463
	χ^2	0.0069	0.0072	0.0057	0.0033	0.0039	0.0055
	SSE	0.0006	0.0006	0.0005	0.0003	0.0003	0.0005
50	a (mg/min mg)	0.1081	0.0921	0.0715	0.0688	0.0679	0.0508
	b (mg/mg)	26.7380	24.3902	23.4192	21.5517	23.5294	25.5754
	R^2	0.8341	0.8953	0.9529	0.9660	0.9566	0.9779
	χ^2	0.0195	0.0181	0.0072	0.0056	0.0071	0.0035
	SSE	0.0029	0.0027	0.0010	0.0009	0.0009	0.0005

The intraparticle diffusion model, also known as the Weber-Morris model, is commonly used to describe the internal diffusion of adsorbates within the adsorbent as the rate determining step (Wang & Guo 2020). The typical fitting of the intraparticle model is presented in Figure 3. It can be observed that the plot consists of two linear lines. The parameters for the intraparticle diffusion model in this study are presented in Tables 7 and 8 for the first and second linear section of the model, respectively. It can be discerned that in all experiment conditions the C values are nonzero. The presence of two linear lines and nonzero C values mean that the rate determining steps in this study are both intraparticle and film diffusion (An 2020). Further comparison of the intraparticle diffusion constant in the first (k_d1) and second (k_d2) linear section shows that the k_d1 values are bigger than k_d2. This indicates that the film diffusion during the adsorption process was more rapid compared with the intraparticle diffusion (Ohale *et al.* 2020). A similar trend in coagulation studies has also been reported previously (Okey-Onyesolu *et al.* 2020).

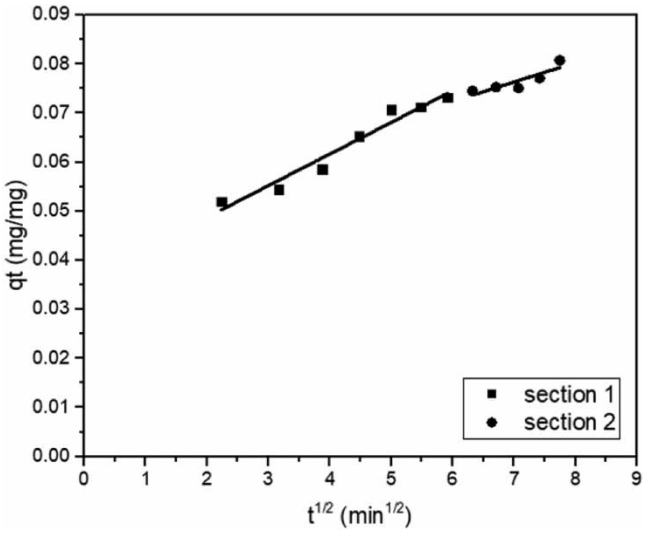

Figure 3 | Typical plot of intraparticle diffusion model (30 °C, 50 mg/L).

Table 7 | Parameters of intraparticle diffusion model section 1

		Initial concentration (mg/L)					
T (°C)	Parameter	50	60	70	80	90	100
30	k_d1 (/min$^{1/2}$)	0.0064	0.0078	0.0077	0.0057	0.0051	0.0093
	C	0.0359	0.0431	0.0473	0.0554	0.0650	0.0504
	R^2	0.9569	0.9728	0.9906	0.9322	0.8812	0.9518
	χ^2	0.0018	0.0026	0.0025	0.0008	0.0008	0.0025
	SSE	0.0001	0.0002	0.0002	0.0001	0.0001	0.0003
40	k_d1 (/min$^{1/2}$)	0.0114	0.0090	0.0104	0.0175	0.0134	0.0111
	C	0.0408	0.0534	0.0473	0.0133	0.0366	0.0506
	R^2	0.8238	0.9430	0.9497	0.9315	0.9803	0.9899
	χ^2	0.0195	0.0031	0.0076	0.0283	0.0113	0.0049
	SSE	0.0019	0.0003	0.0008	0.0031	0.0013	0.0006
50	k_d1 (/min$^{1/2}$)	0.0103	0.0139	0.0164	0.0226	0.0181	0.0194
	C	0.1150	0.1007	0.0793	0.0600	0.0697	0.0421
	R^2	0.9058	0.9617	0.9259	0.9720	0.9574	0.9183
	χ^2	0.0062	0.0076	0.0058	0.0231	0.0103	0.0177
	SSE	0.0011	0.0014	0.0010	0.0044	0.0018	0.0026

The agreement of experimental and model data was evaluated by the R^2, χ^2, and SSE values. It can be observed that all kinetic models gave relatively high R^2 values around 0.8–0.9, except for the fitting of the second section intra-particle model. Among all kinetic models, it can also be seen that the pseudo-second order model showed

Table 8 | Parameters of intraparticle diffusion model section 2

T (°C)	Parameter	Initial concentration (mg/L)					
		50	60	70	80	90	100
30	k_d2 (/min$^{1/2}$)	0.0040	0.0025	0.0025	0.0033	0.0038	0.0021
	C	0.0486	0.0746	0.0776	0.0754	0.0766	0.0954
	R^2	0.7717	0.9231	0.9479	0.9085	0.8037	0.9323
	X^2	0.0021	0.0127	0.0105	0.0100	0.0035	0.0247
	SSE	0.0001	0.0009	0.0007	0.0008	0.0003	0.0020
40	k_d2 (/min$^{1/2}$)	0.0014	0.0019	0.0036	0.0051	0.0020	0.0051
	C	0.0937	0.0991	0.0835	0.0779	0.1025	0.0825
	R^2	0.8744	0.8787	0.4768	0.8770	0.7906	0.7770
	X^2	0.0341	0.0207	0.0120	0.0574	0.0452	0.0078
	SSE	0.0020	0.0016	0.0009	0.0027	0.0034	0.0006
50	k_d2 (/min$^{1/2}$)	0.0029	0.0024	0.0069	0.0053	0.0132	0.0113
	C	0.1543	0.1666	0.1343	0.1544	0.0862	0.0781
	R^2	0.9230	0.9134	0.9286	0.9512	0.9176	0.8801
	X^2	0.0078	0.0241	0.0210	0.0517	0.0037	0.0126
	SSE	0.0011	0.0033	0.0025	0.0060	0.0006	0.0011

$R^2 > 0.99$ with very low χ^2 and SSE values and good fit of model and experimental data as presented in Figure 4. This indicates the pseudo-second order model was the most suitable model to describe the coagulation kinetic in this study. The use of pseudo-second order kinetic model to describe the coagulation process has also been reported by previous researchers (Obiora-Okafo *et al.* 2019; Ngteni *et al.* 2020; Okey-Onyesolu *et al.* 2020). The suitability to the pseudo-second order kinetic model indicates that the coagulation process is chemisorption in nature, due to the interaction between coagulant and Congo red molecules via hydrogen or dipole-dipole bonds (Jadhav & Mahajan 2014).

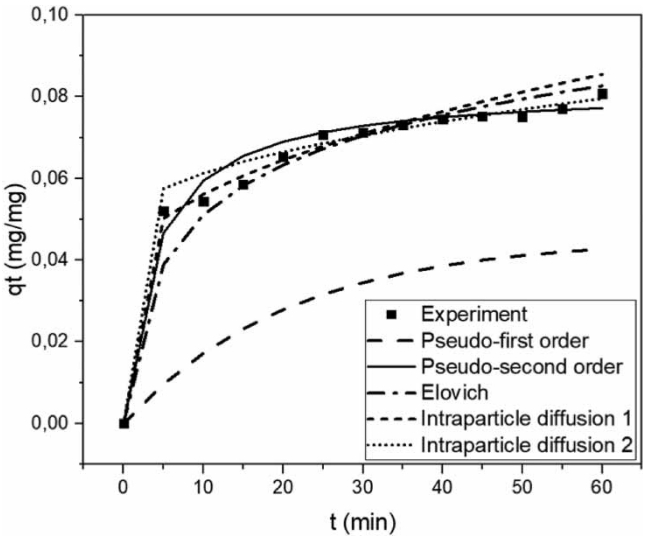

Figure 4 | Comparison of experiment and model data (30 °C, 50 mg/L).

Isotherm adsorption

The parameters of various isotherm adsorption models, namely the Langmuir, Freundlich, Temkin, and BET models, are presented in Table 9. The Langmuir model assumes a homogeneous adsorption phenomenon with constant enthalpy of each molecule. The Langmuir constant (K_L) illustrates the adsorption capacity of the coagulant. It can be seen that with the increase of temperature, the K_L values also increased. Furthermore, the calculated separation factor (R_L) ranged from 0.169 to 0.289, 0.047 to 0.090, and 0.006 to 0.012 for coagulation

Table 9 | Parameters of isotherm adsorption models

Langmuir					
Temperature	**KL (L/mg)**	**qm (mg/mg)**	**R^2**	**χ^2**	**SSE**
30 °C	0.0492	0.1432	0.9408	3.5×10^{-4}	3.4×10^{-5}
40 °C	0.2019	0.1307	0.8769	2.3×10^{-4}	2.7×10^{-5}
50 °C	1.6650	0.1940	0.8645	1.5×10^{-4}	3.0×10^{-5}
Freundlich					
Temperature	**KF (L/mg)**	**1/n**	**R^2**	**χ^2**	**SSE**
30 °C	0.0294	0.3148	0.9304	4.1×10^{-4}	3.8×10^{-5}
40 °C	0.0739	0.1210	0.8440	2.7×10^{-4}	3.1×10^{-5}
50 °C	0.1651	0.0410	0.7750	2.4×10^{-4}	4.5×10^{-5}
Temkin					
Temperature	**A (L/mg)**	**b (J/mol)**	**R^2**	**χ^2**	**SSE**
30 °C	0.5714	8.34×10^4	0.9419	3.7×10^{-4}	3.5×10^{-5}
40 °C	114.1172	1.90×10^5	0.8470	2.7×10^{-4}	3.0×10^{-5}
50 °C	3.22×10^9	3.58×10^5	0.7683	2.3×10^{-4}	4.4×10^{-5}
BET					
Temperature	**A**	**Xm (mg/mg)**	**R^2**	**χ^2**	**SSE**
30 °C	−3.5234	0.0293	0.9148	0.0010	8.6×10^{-5}
40 °C	−2.7752	0.0346	0.9745	0.0021	2.3×10^{-4}
50 °C	−13.3093	0.0979	0.9673	0.1040	1.8×10^{-2}

temperature of 30°, 40°, and 50 °C, respectively. The R_L values ranging between $0 < R_L < 1$ indicate a favourable adsorption, while the decreasing trend of R_L indicates an increased affinity between Congo red molecules and leucaena protein during the coagulation (Lin *et al.* 2011).

The Freundlich model is based on the assumption that adsorption of multi-layered adsorbates on heterogeneous adsorbent surfaces with different energy levels. The Freundlich constant, K_F (L/mg), illustrates the relation between adsorbate and adsorbent as well as the adsorption capacity. It can be inferred from Table 8 that KF values increased with the increase of coagulation temperature, indicating the increased adsorption capacity with the increase of temperature and the endothermic nature of the coagulation adsorption in this study. Furthermore, the 1/n values fall within the range of $0 < 1/n < 1$ indicating a favourable coagulation adsorption of Congo red dye using leucaena protein.

The Temkin model assumes that heat of adsorption is a function of temperature and linearly decreases due to interaction of adsorbate and adsorbent during the adsorption process (Al-Ghouti & Da'ana 2020). The A value of the Temkin model indicates the binding energy. The increase of A values with the increase of coagulation temperature confirmed the endothermic nature of Congo red coagulation adsorption in this study (Aljeboree *et al.* 2017).

The BET adsorption is known as a modification of the Langmuir model. In the BET model, adsorption of dye molecules is randomly distributed and a multilayer adsorbate is formed. There are two parameters in the BET model, namely A, which is the BET constant, and *Xm* (mg/mg), the amount of adsorbed Congo red molecule by the coagulant to form a monolayer (Hossain *et al.* 2019). The increase of X_M values demonstrates the increase of Congo red molecule that was adsorbed in the form of monolayer on the coagulation adsorption process. Furthermore, the negative A values implied that the surface of the coagulant was saturated with the Congo red molecules (Hossain *et al.* 2019).

The suitability of the isotherm adsorption models was examined by observing the R^2, χ^2 and SSE values. It can be seen in Table 8 that in terms of R^2, the BET model gave the highest R^2 compared to other models. However, based on the fitting of experimental and model data as seen in Figure 5, the BET model turned out to be the least suitable of the four models. Furthermore, it can be observed that the Langmuir model gave the smallest χ^2 and SSE values, confirming the suitability of the Langmuir model in this study. Thus, it is safe to conclude that the coagulation adsorption of Congo red by leucaena protein occurred in a form of monolayer and on a homogenous surface. The suitability of the Langmuir model to describe the coagulation using natural coagulant has also been reported by previous researchers (Antov *et al.* 2010; Kebaili *et al.* 2018; Menkiti *et al.* 2018).

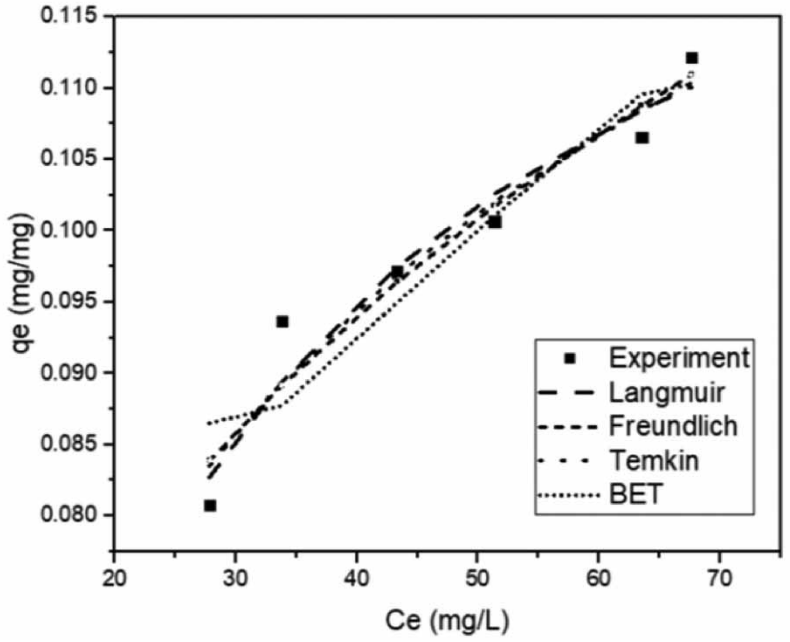

Figure 5 | Suitability of several isotherm model with experimental data (T = 30 °C).

Thermodynamics

The thermodynamic parameters of Congo red coagulation adsorption in this study are presented in Table 10. It shows that at all coagulation temperatures the $\Delta G°$ values were negative, indicating the spontaneous nature of the coagulation process. The increase of $\Delta G°$ negativity with the increase of coagulation temperature indicated the increase of spontaneity at higher temperature. Furthermore, it can be discerned that the positive $\Delta S°$ indicated the randomness of the interaction of Congo red and leucaena protein during the coagulation process. The magnitude of $\Delta H°$ value could be used to infer whether the coagulation adsorption process was physisorption ($\Delta H° <$ 40 kJ/mol) or chemisorption ($\Delta H° > 40$ kJ/mol) (Egbosiuba *et al.* 2020). The $\Delta H°$ value of 142.96 kJ/mol suggested that the Congo red coagulation was more a matter of chemisorption than physisorption. Furthermore, the positive value of $\Delta H°$ confirmed the endothermic characteristic of Congo red coagulation adsorption.

Table 10 | Thermodynamic parameters of Congo red coagulation

	Parameter		
Temperature (°C)	**ΔG° (kJ/mol)**	**ΔH° (kJ/mol)**	**ΔS° (kJ/mol K)**
30	−36.32	142.96	0.45
40	−41.20		
50	−48.18		

Coagulant cost evaluation

To evaluate the possible application of leucaena crude extract as a natural coagulant to substitute for inorganic chemical coagulant, its economic aspects and feasibility were analysed. Calculation of coagulant cost was based on the ingredients that were needed to obtain the coagulant, disregarding other costs such as energy, labor, depreciation of capital cost, and the like. In the preparation of leucaena extract, the contributing cost consists of leucaena seeds ($3.45/kg), NaCl, and distilled water. Calculation was based on the optimum coagulation dosage for 50 mg/L Congo red removal was found to be 10 mL/L using leucaena extract (Kristianto *et al.* 2019), compared with ferrous sulphate (159.64 mg/L) (Luo *et al.* 2019) and aluminium sulphate (40 mg/L) (Goudjil *et al.* 2021). The cost was estimated taking into consideration that the leucaena seed kernel amounted to 50%-w of the total seeds weight (Sethi & Kulkarni 1995), and chemical cost was derived from a marketplace in Indonesia. Based on the estimated cost presented in Table 11, it could be observed that utilization of leucaena extract as natural coagulant was the most expensive, compared to ferrous sulphate and aluminium sulphate. The high cost comes from utilization of NaCl and distilled water for protein extraction that accounts for up to 85% of the cost. A similar observation was reported by Ang, Kiatkittipong (Ang *et al.* 2020), namely that the extraction process would contribute greatly to the natural coagulant cost. The higher natural coagulant cost compared to inorganic coagulant has also been reported by other researchers (Zheng *et al.* 2021). However, despite the high cost, the use of the natural coagulant was worthwhile because of the environmental and social impact of the natural coagulant's life cycle analysis, which has been reported to be better than inorganic coagulants' (Niquette *et al.* 2004; Zheng *et al.* 2021). It is generally known that environmental and social impact, as well as economic aspects, are important factors in achieving the actual sustainability of a process. Further optimization of the extraction process is needed to minimize the cost of natural coagulant from leucaena seeds.

Table 11 | Cost estimation of leucaena extract compared to inorganic coagulants for treating 50 mg/L Congo red wastewater

Coagulant	Optimal dosage	Estimated cost ($/m^3)
leucaena extract	10 mL/L	24.09
ferrous sulphate	159.64 mg/L	16.54
aluminium sulphate	40 mg/L	2.58

CONCLUSION

This study has investigated the effect of Congo red concentration and temperature on the coagulation performance of leucaena crude extract. It was found that both variables and their interaction were significant to the removal of Congo red. Furthermore, the coagulation process was investigated by using several adsorption kinetic and isotherm models. It was found that the sedimentation process was well described by the pseudo-second order kinetic model, indicating chemisorption of Congo red on the coagulant. From the intraparticle model, it could be inferred that both intraparticle and film diffusion were the determining steps, where the latter was more dominant in the diffusion process. The experimental data using isotherm models show that the Langmuir model is the best model to describe the coagulation process, inferring the monolayer adsorption process in this study. Furthermore, based on the thermodynamic parameters, it was found that the coagulation was spontaneous and endothermic in nature. The results of this study show that leucaena extract could be used as alternative coagulant to treat colour wastewater. Further study to optimize the extraction process to lower the coagulant cost and further application in more complex wastewater are needed, prior to its commercial application.

ACKNOWLEDGEMENTS

This study is funded by Parahyangan Catholic University's Centre of Research and Community Service under contract No III/LPPM/2022-02/34-P. The authors are grateful for the financial support provided.

CONFLICT OF INTEREST STATEMENT

The authors declare they have no competing interests.

DATA AVAILABILITY STATEMENT

Data cannot be made publicly available; readers should contact the corresponding author for details.

REFERENCES

Ahmad, A., Abdullah, S. R. S., Hasan, H. A., Othman, A. R. & Ismail, N. I. 2021 Plant-based versus metal-based coagulants in aquaculture wastewater treatment: effect of mass ratio and settling time. *J. Water Process Eng.* **43**, 102269.

Al-Ghouti, M. A. & Da'ana, D. A. 2020 Guidelines for the use and interpretation of adsorption isotherm models: a review. *J. Hazard. Mater.* **393**, 122383.

Aljeboree, A. M., Alshirifi, A. N. & Alkaim, A. F. 2017 Kinetics and equilibrium study for the adsorption of textile dyes on coconut shell activated carbon. *Arabian J. Chem.* **10**, S3381–S3393.

An, B. 2020 Cu(II) and As(V) adsorption kinetic characteristic of the multifunctional Amino groups in Chitosan. *Processes* **8**, 1194.

Ang, W. L. & Mohammad, A. W. 2020 State of the art and sustainability of natural coagulants in water and wastewater treatment. *J. Cleaner Prod.* **262**. Article No 121267.

Ang, T.-H., Kiatkittipong, K., Kiatkittipong, W., Chua, S.-C., Lim, J. W., Show, P.-L., Bashir, M. & Ho, Y.-C. 2020 Insight on extraction and characterisation of biopolymers as the green coagulants for microalgae harvesting. *Water* **12**. Article No 1388.

Antov, M. G., Šciban, M. B. & Petrovic, N. J. 2010 Proteins from common bean (Phaseolus vulgaris) seed as a natural coagulant for potential application in water turbidity removal. *Bioresour. Technol.* **101**, 2167–2172.

Beltran-Heredia, J., Sanchez-Martın, J. & Delgado-Regalado, A. 2009 Removal of carmine indigo dye with Moringa oleifera seed extract. *Ind. Eng. Chem. Res.* **48**, 6512–6520.

Bradford, M. M. 1976 A rapid and sensitive method for the quantitation of microgram quantities of protein utilizing the principle of protein-dye binding. *Anal. Biochem.* **72**, 248–254.

Crini, G. & Lichtfouse, E. 2019 Advantages and disadvantages of techniques used for wastewater treatment. *Environ. Chem. Lett.* **17**, 145–155.

Egbosiuba, T. C., Abdulkareem, A. S., Kovo, A. S., Afolabi, E. A., Tijani, J. O., Auta, M. & Roos, W. D. 2020 Ultrasonic enhanced adsorption of methylene blue onto the optimized surface area of activated carbon: adsorption isotherm, kinetics and thermodynamics. *Chem. Eng. Res. Des.* **153**, 315–336.

Ejimofor, M. I., Ezemagu, I. G., Ugonabo, V. I., Nnaji, P. C., Anadebe, V. C., Diyoke, C. & Menkiti, M. C. 2022 Adsorption kinetics, mechanistic, isotherm and thermodynamics study of petroleum produced water coagulation using novel Egeria radiate shell extract (ERSE). *J. Indian Chem. Soc.* **99**(3), 100357.

Fitzpatrick, C. S. B., Fradin, E. & Gregory, J. 2004 Temperature effects on flocculation, using different coagulants. *Water Sci. Technol.* **50**(12), 171–175.

Goudjil, S., Guergazi, S., Masmoudi, T. & Achour, S. 2021 Effect of reactional parameters on the elimination of Congo Red by the combination of coagulation–floculation with aluminum sulfate. *Desalin. Water Treat.* **209**, 429–436.

He, Q. & Xie, M. 2021 Thermodynamic analysis of Brownian motion-induced particle agglomeration using the Taylor-series expansion method of moments. *Processes* **9**, 1218.

Hossain, M. S., Omar, F., Asis, A. J., Bachmann, R. T., Sarker, M. Z. I. & Kadir, M. O. 2019 Effective treatment of palm oil mill effluent using FeSO4.7H2O waste from titanium oxide industry: coagulation adsorption isotherm and kinetics studies. *J. Cleaner Prod.* **219**, 86–98.

Hussain, S., Leeuwen, J. v., Chow, C., Beecham, S., Kamruzzaman, M., Wang, D., Drikas, M. & Aryal, R. 2013 Removal of organic contaminants from river and reservoir waters by three different aluminum-based metal salts: coagulation adsorption and kinetics studies. *Chem. Eng. J.* **225**, 394–405.

Jadhav, M. V. & Mahajan, Y. S. 2014 Assessment of feasibility of natural coagulants in turbidity removal and modeling of coagulation process. *Desalin. Water Treat.* **52**(31–33), 5812–5821.

Kebaili, M., Djellali, S., Radjai, M., Drouiche, N. & Lounici, H. 2018 Valorization of orange industry residues to form a natural coagulant and adsorbent. *J. Ind. Eng. Chem.* **64**, 292–299.

Kristanda, J., Sintiago, K. S., Kristianto, H., Prasetyo, S. & Sugih, A. K. 2021 Optimization study of Leucaena leucocephala seeds extract as natural coagulant on decolorization of aqueous Congo red solutions. *Arabian J. Sci. Eng.* **46**(7), 6275–6286.

Kristianto, H., Paulina, S. & Soetedjo, J. N. M. 2018 Exploration of various Indonesian indigenous plants as natural coagulant for synthetic turbid water. *IJTech* **9**(3), 464–471.

Kristianto, H., Rahman, H., Prasetyo, S. & Sugih, A. K. 2019 Removal of Congo red aqueous solution using Leucaena leucocephala seed's extract as natural coagulant. *Appl. Water Sci.* **9**(4). Article No 88.

Kristianto, H., Tanuarto, M. Y., Prasetyo, S. & Sugih, A. K. 2020a Magnetically assisted coagulation using iron oxide nanoparticles – Leucaena leucocephala seeds' extract to treat synthetic Congo red wastewater. *Int. J. Environ. Sci. Technol.* **17**(7), 3561–3570.

Kristianto, H., Reynaldi, E., Prasetyo, S. & Sugih, A. K. 2020b Adsorbed Leucaena protein on citrate modified Fe3O4 nanoparticles: synthesis, characterization, and its application as magnetic coagulant. *Sustainable Environ. Res.* **30**, 32.

Kristianto, H., Saraswati, S. A., Prasetyo, S. & Sugih, A. K. 2022 The utilization of galactomannan from spent coffee grounds as a coagulant aid for treatment of synthetic Congo red wastewater. *Environ. Dev. Sustainable.* In-press.

Lal, K. & Garg, A. 2017 Physico-chemical treatment of pulping effluent: characterization of flocs and sludge generated after treatment. *Sep. Sci. Technol.* **52**(9), 1583–1593.

Lal, K. & Garg, A. 2019 Effectiveness of synthesized aluminum and iron based inorganic polymer coagulants for pulping wastewater treatment. *J. Environ. Chem. Eng.* **7**, 103204.

Lima, E. C., Hosseini-Bandegharaei, A., Moreno-Pirajá, J. C. & Anastopoulos, I. 2019 A critical review of the estimation of the thermodynamic parameters on adsorption equilibria. wrong use of equilibrium constant in the Van't Hoof equation for calculation of thermodynamic parameters of adsorption. *J. Mol. Liq.* **273**, 425–434.

Lin, J., Zhan, Y. & Zhu, Z. 2011 Adsorption characteristics of copper (II) ions from aqueous solution onto humic acid-immobilized surfactant-modified zeolite. *Colloids Surf. A* **384**, 9–16.

Luo, X., Liang, C. & Hu, Y. 2019 Comparison of different enhanced coagulation methods for azo dye removal from wastewater. *Sustainability* **11**(17), 4760.

Mahmoudabadi, T. Z., Abbasi, F., Jalili, M. & Talebi, P. 2019 Effectiveness of Plantago major extract as a natural coagulant in removal of reactive blue 19 dye from wastewater. *Int. J. Environ. Sci. Technol.* **16**, 7893–7900.

Menkiti, M. C., Okoani, A. O. & Ejimofor, M. I. 2018 Adsorptive study of coagulation treatment of paint wastewater using novel Brachystegia eurycoma extract. *Appl. Water Sci.* **8**, 189.

Ngteni, R., Hossain, M. S., Kadir, M. O. A., Asis, A. J. & Tajudin, Z. 2020 Kinetics and isotherm modeling for the treatment of rubber processing effluent using iron (II) sulphate waste as a coagulant. *Water* **12**, 1747.

Niquette, P., Monette, F., Azzouz, A. & Hausler, R. 2004 Impacts of substituting aluminum-Based coagulants in drinking water treatment. *Water Qual. Res. J. Can.* **39**(3), 303–310.

Nnaji, P. C., Anadebe, V. C., Ezemagu, I. G. & Onukwuli, O. D. 2022 Potential of Luffa cylindrica seed as coagulation-flocculation (CF) agent for the treatment of dye wastewater: kinetic, mass transfer, optimization and CF adsorption studies. *Arabian J. Chem.* **15**(2), 103629.

Obiora-Okafo, I. A., Onukwuli, O. D. & Ezugwu, C. N. 2019 Application of kinetics and mathematical modelling for the study of colour removal from aqueous solution using natural organic polymer. *Desalin. Water Treat.* **165**, 362–373.

Obiora-Okafo, I. A., Onukwuli, O. D. & Eli-Chukwu, N. C. 2020 Evaluation of bio-coagulants for colour removal from dye synthetic wastewater: characterization, adsorption kinetics, and modelling approach. *Water SA* **46**(2), 300–312.

Ohale, P. E., Onu, C. E., Ohale, N. J. & Oba, S. N. 2020 Adsorptive kinetics, isotherm and thermodynamic analysis of fishpond effluent coagulation using chitin derived coagulant from waste Brachyura shell. *Chem. Eng. J. Adv.* **4**, 100036.

Okey-Onyesolu, C. F., Onukwuli, O. D., Ejimofor, M. I. & Okoye, C. C. 2020 Kinetics and mechanistic analysis of particles decontamination from abattoir wastewater (ABW) using novel Fish Bone Chito-protein (FBC). *Heliyon* **6**, e04468.

Okolo, B. I., Adeyi, O., Oke, E. O., Agu, C. M., Nnaji, P. C., Akatobi, K. N. & Onukwuli, D. O. 2021 Coagulation kinetic study and optimization using response surface methodology for effective removal of turbidity from paint wastewater using natural coagulants. *Sci. Afr.* e00959. In Press.

Patel, H. & Vashi, R. T. 2012 Removal of Congo Red dye from its aqueous solution using natural coagulants. *J. Saudi Chem. Soc.* **16**, 131–136.

Qiu, H., Lv, L., Pan, B., Zhang, Q., Zhang, W. & Zhang, Q. 2009 Critical review in adsorption kinetic models. *J. Zhejiang Univ. Sci. A* **10**(5), 716–725.

Rani, C. N. & Talikoti, R. 2013 Adsorption isotherm studies of the simultaneous removal of turbidity and hardness by natural coagulants. *Water Pract. Technol.* **8**(3–4), 495–502.

Rodrigues, C. S. D., Madeira, L. M. & Boaventura, R. A. R. 2013 Treatment of textile dye wastewaters using ferrous sulphate in a chemical coagulation/flocculation process. *Environ. Technol.* **34**(6), 719–729.

Sethi, P. & Kulkarni, P. R. 1995 Leucaena leucocephala: a nutrition profile. *Food Nutr. Bull.* **16**(3), 1–16.

Thirugnanasambandham, K. & Karri, R. R. 2021 Preparation and characterization of Azadirachta indica A. Juss. plant based natural coagulant for the application of urban sewage treatment: modelling and cost assessment. *Environ. Technol. Innovation* **23**, 101733.

Verma, A. K., Dash, R. R. & Bhunia, P. 2012 A review on chemical coagulation/flocculation technologies for removal of colour from textile wastewaters. *J. Environ. Manage.* **93**, 154–168.

Vishali, S. & Karthikeyan, R. 2018 Application of green coagulants on paint industry effluent – a coagulation– flocculation kinetic study. *Desalin. Water Treat.* **122**, 112–123.

Vishali, S., Sakthivel, S., Karthick, R. & Gowsigan, V. S. 2020 A sustainable approach for the treatment of industrial effluent using a green coagulant Cassia fistula vs. chemical coagulant. *Desalin. Water Treat.* **196**, 189–197.

Vishali, S., Mullai, P., Mahboob, S., Al-Ghanim, K. & Sivasankar, A. 2022 Elucidation the influence of design variables on coagulation–flocculation mechanisms in the lab-scale bio-coagulation on toxic industrial effluent treatment. *Environ. Res.* **212**, 113224.

Wang, J. & Guo, X. 2020 Adsorption kinetic models: physical meanings, applications, and solving methods. *J. Hazard. Mater.* **390**, 122156.

Wu, Z., Zhang, X., Pang, J., Li, J., Li, J. & Zhang, P. 2020 High-poly-aluminum chloride sulfate coagulants and their coagulation performances for removal of humic acid. *RSC Adv.* **10**, 7155–7162.

Yamaguchi, N. U., Cusioli, L. F., Quesada, H. B., Ferreira, M. E. C., Fagundes-Klen, M. R., Vieira, A. M. S., Gomes, S. G., Vieira, M. F. & Bergamasco, R. 2021 A review of Moringa oleifera seeds in water treatment: trends and future challenges. *Process Saf. Environ. Prot.* **147**, 406–420.

Yasin, N. M. F. M., Hossain, M. S., Abdul Khalil, H. P. S., Zulkifli, M., Al-Gheethi, A., Asis, A. J. & Yahaya, A. N. A. 2020 Treatment of palm oil refinery effluent using tannin as a polymeric coagulant: isotherm, kinetics, and thermodynamics analyses. *Polymers* **12**(10), 2353.

Yin, C.-Y. 2010 Emerging usage of plant-based coagulants for water and wastewater treatment. *Process Biochem.* **45**, 1437–1444.

Zheng, W. C., Ismail, N., Boboi, C. O. & Lin, C. B. 2021 Life cycle analysis for Hibiscus Sabdariffa powder manufactured by freeze drying for wastewater application. *MATEC Web Conf.* **335**, 01002.

Zhou, X. & Zhou, X. 2014 The unit problem in the thermodynamic calculation of adsorption using the Langmuir equation. *Chem. Eng. Commun.* **201**(11), 1459–1467.

First received 25 February 2022; accepted in revised form 13 May 2022. Available online 25 May 2022